Some Consideration on Derivative Approximation of Particle Methods

Hitoshi Matsubara, Shigeo Iraha, Genki Yagawa and Doosam Song

Abstract In this paper, the accuracy of the derivative approximation of the particle methods is discussed. Especially, we show that the issue of decreasing accuracy on a boundary area in the SPH method is due to the lack of the boundary integration. Through some numerical examples, the convergence of error norm of energy obtained by the SPH and the MPS methods is studied.

1 Introduction

The advantage of the particle methods lies in the fact that no cost is needed in mesh generation contrary to the usual finite element methods [1], although there have been several studies to remove this bottleneck of the finite element methods. It is well known that the particle or the node based methods [2–6] have the following merits [7]:

(a) Simulations of very large deformations can be easily handled.
(b) The data structure of particle or node discretization can be linked easily with the CAD database.
(c) The adaptive refinement procedure can be easily controlled.
(d) The mesh-free discretization provides accurate representation of the geometry of the objects to be solved.

Hitoshi Matsubara · Shigeo Iraha
Department of Civil Engineering and Archtecture, University of the Ryukyus, 1, Senbaru, Nishihara, Okinawa 903-0213, Japan; e-mail: {matsbara, iraha}@tec.u-ryukyu.ac.jp

Genki Yagawa
Center for Computational Mechanics Research, Tokyo University, 2-36-5, Hakusan, Bunkyo-ku, Tokyo 112-0001, Japan; e-mail: yagawa@eng.toyo.ac.jp

Doosam Song
School of Architecture, Sungkyunkwan University, 300 Cheoncheon, Suwon 440-746, Korea; e-mail: dssong@skku.edu

E. Oñate and R. Owen (eds.), *Particle-Based Methods*, Computational Methods in Applied Sciences 25, DOI 10.1007/978-94-007-0735-1_9,
© Springer Science+Business Media B.V. 2011

Lucy [8] and Gingold and Monaghan [9] originated the smoothed particle hydrodynamics (SPH) for astrophysical computations, which is a purely Lagrangian description and has been extended to solve a wide range of issues in physics or engineering fields. Today, SPH is being extensively applied to simulations of supernovas, collapse as well as formation of galaxies [7], also SPH has been extended to treat the incompressive flow problems or the solid mechanics [11]. Concerning the accuracy improvements of SPH, Belytschko et al. [12] examined corrected first derivative approximations, where the proposed approximations restored the accuracy in various benchmark problems, but establishment of the complete approximation was not reached because of the lack of integrability. On the other hand, Libersky et al. [13,14] introduced ghost particles to reflect a symmetrical surface boundary condition. Recently, Chen et al. [15–17] proposed a simple corrective kernel approximation by applying the kernel estimate to the Taylor series expansion. By using these modified numerical techniques, the derivative approximation of SPH is improved dramatically. However, the problem of the accuracy issue on the boundary or the edge of the object is not completely solved even if we use the above techniques.

A similar particle approach is called the moving particle semi-implicit (MPS) method [18–21], which is based on the Lagrangian description. In this method, the differential operators such as the gradient and Laplacian in the governing equations are previously-prepared in an intuitive manner. The general accuracy in this method remains to be clarified.

As discussed in the above, the accuracy of the derivative approximation of the particle methods is one of the most important issues, and the accuracy on the boundary or the edge remains to be solved in particular. One of the reasons might be due to the fact that we cannot calculate boundary integrals precisely because there is no definite or exact boundary in the particle methods.

In this study, we study the accuracy of the derivative approximation for SPH and MPS methods. Particularly, concerning the accuracy at the boundary or the edge of the body to be solved, we theoretically examine the discretization formulation especially for SPH. Then, the present paper aims to discuss the influence of number of particles or particle distributions on the accuracy of SPH and MPS method through some numerical examples.

2 Formulation and Some Remarks on Particle Methods

In the so-called Smoothed Particle Hydrodynamics or SPH method, the continuum is assumed to be a collection of particles, and its density, velocity, stresses etc. are evaluated through the particle-wise manner. Its interpolation is based on the following concept of kernel estimate:

$$f(\mathbf{x}) \cong \int_{\Re} f(\mathbf{x}')w(\mathbf{x}-\mathbf{x}')d\Omega_{\mathbf{x}'}, \quad \mathbf{x} \in \Re \tag{1}$$

where $f(\mathbf{x})$ is an a vector function of the three-dimentional position vector $\mathbf{x}$ and $w(\mathbf{x}-\mathbf{x}')$ is the kernel function selected to be zero beyond the interaction area. The approximation for spatial derivatives is obtained by substituting $\nabla \cdot f(\mathbf{x})$ for $f(\mathbf{x})$ in Equation (1) as follows:

$$\nabla \cdot f(\mathbf{x}) \cong \int_{\Re} \nabla \cdot f(\mathbf{x}')w(\mathbf{x}-\mathbf{x}')d\Omega_{\mathbf{x}'} \tag{2}$$

The divergence of the above equation is given as [22]

$$\nabla \cdot f(\mathbf{x}) \cong \int_{\Re} \nabla \left(f(\mathbf{x}')w(\mathbf{x}-\mathbf{x}')\right) d\Omega_{\mathbf{x}'} - \int_{\Re} f(\mathbf{x}')\nabla \cdot w(\mathbf{x}-\mathbf{x}')d\Omega_{\mathbf{x}'} \tag{3}$$

The first term of the right-hand side of Equation (3) can be converted by means of the divergence theorem into an integral over the surface of the domain of integration as follows:

$$\int_{\Re} \nabla \left(f(\mathbf{x}')w(\mathbf{x}-\mathbf{x}')\right) d\Omega_{\mathbf{x}'} = \int_{s} f(\mathbf{x}')w(\mathbf{x}-\mathbf{x}')ds \tag{4}$$

The surface integral becomes zero because the kernel function $w(\mathbf{x}-\mathbf{x}')$ is zero on the boundaries. Therefore, the approximation for spatial derivatives of $f(\mathbf{x})$ is defined as

$$\nabla \cdot f(\mathbf{x}) \cong -\int_{\Re} f(\mathbf{x}')\nabla \cdot w(\mathbf{x}-\mathbf{x}')d\Omega_{\mathbf{x}'} \tag{5}$$

Based on the above-mentioned theoretical background, we can obtain the following equations as the SPH discretization:

$$f(\mathbf{x}) = \sum_{j=1}^{N} \frac{m_j}{\rho_j} f(\mathbf{x}_j)w(\mathbf{x}-\mathbf{x}_j) \tag{6}$$

$$\nabla \cdot f(\mathbf{x}) = -\sum_{j=1}^{N} \frac{m_j}{\rho_j} f(\mathbf{x}_j)\nabla \cdot w(\mathbf{x}-\mathbf{x}_j) \tag{7}$$

where N is the number of particles in an interaction area, m_j is the mass of particle j and ρ_j is defined as

$$\rho_j = \sum_{k=1}^{N} m_k w(\mathbf{x}-\mathbf{x}_k) \tag{8}$$

On the other hand, a modified kernel [15–17], which is resulted by dividing Equations (6) and (7) by the sum total of kernel function, has been proposed in order to improve the accuracy of discretization as shown in the following equations:

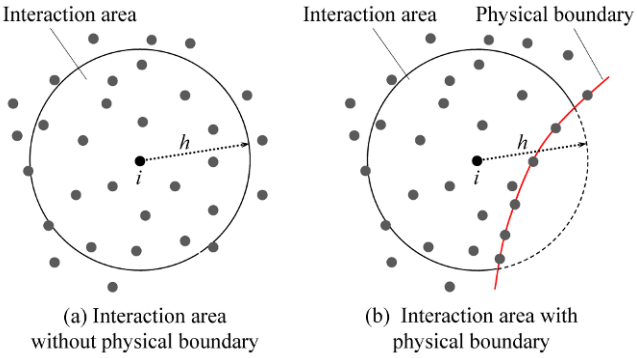

Fig. 1 Interaction area around particle i (h: radius of interaction area)

$$f(\mathbf{x}) = \frac{\sum_{j=1}^{N} \frac{m_j}{\rho_j} f(\mathbf{x}_j) w(\mathbf{x} - \mathbf{x}_j)}{\sum_{j=1}^{N} \frac{m_j}{\rho_j} w(\mathbf{x} - \mathbf{x}_j)} \tag{9}$$

$$\nabla \cdot f(\mathbf{x}) = -\frac{\sum_{j=1}^{N} \frac{m_j}{\rho_j} f(\mathbf{x}_j) \nabla \cdot w(\mathbf{x} - \mathbf{x}_j)}{\sum_{j=1}^{N} \frac{m_j}{\rho_j} \nabla \cdot w(\mathbf{x} - \mathbf{x}_j)} \tag{10}$$

In the SPH method, Equations (6), (7), (9) and (10) are directly employed for calculations. It is here noted that these equations can be used only when the conversion from Equation (3) to Equation (5) is valid. In other words, we should be careful if these are applied to the continuum with a boundary. Or this conversion is valid only in cases where there are no physical boundaries in the interaction area as shown in Figure 1a, and we cannot apply this conversion to the interaction area with physical boundaries as shown in Figure 1b. There will be some effects on the accuracy of results in the continuum with physical boundaries, although the effects are not an issue in such applications as the astro-dynamics, which treat unbounded body.

Thus, in the interaction area with physical boundary as shown in Figure 1b, we must employ the following equation:

$$\nabla \cdot f(x) \cong \int_s f(\mathbf{x}') w(\mathbf{x} - \mathbf{x}') ds - \int_{\Re} f(\mathbf{x}') \nabla \cdot w(\mathbf{x} - \mathbf{x}') d\Omega_{\mathbf{x}'} \tag{11}$$

As shown in the above equation, the boundary integration is an indispensable term in the interaction area with physical boundary, and we need the boundary mesh in order to perform this integration.

In the Moving Particle Semi-implicit or MPS method [18], the gradient vector of an arbitrary particle i is defined as the weighted averaging "gradient model" between

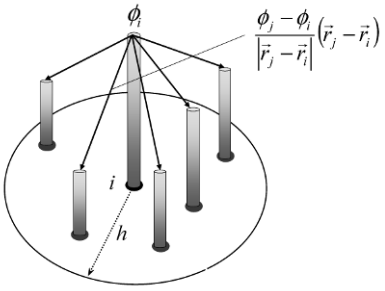

Fig. 2 Evaluation of gradient at particle i in MPS method (h: radius of interaction area)

the particles in the interaction area. Let us assume that particle i and particle j has positional vectors r_i and r_j, and physical value ϕ_i and ϕ_j, respectively. ϕ_j can be approximated by the Taylor expansion around the particle i as follows:

$$\phi_j = \phi_i + \nabla\phi|_{ij} \cdot \left(\mathbf{r}_j - \mathbf{r}_i\right) \tag{12}$$

$$\nabla\phi|_{ij} \cdot \left(\mathbf{r}_j - \mathbf{r}_i\right) = \phi_j - \phi_i \tag{13}$$

Dividing both sides of Equation (12) by the absolute value of a relative positional vector between particles i and j, the following equation is obtained:

$$\nabla\phi|_{ij} \cdot \frac{\left(\mathbf{r}_j - \mathbf{r}_i\right)}{\left|\mathbf{r}_j - \mathbf{r}_i\right|} = \frac{\phi_j - \phi_i}{\left|\mathbf{r}_j - \mathbf{r}_i\right|} \tag{14}$$

By multiplying the unit vector in the direction of a relative positional vector of particles i and j by both sides of Equation (14), we obtain

$$\langle\nabla\phi\rangle_{ij} = \left[\nabla\phi|_{ij} \cdot \frac{\left(\mathbf{r}_j - \mathbf{r}_i\right)}{\left|\mathbf{r}_j - \mathbf{r}_i\right|}\right] \frac{\left(\mathbf{r}_j - \mathbf{r}_i\right)}{\left|\mathbf{r}_j - \mathbf{r}_i\right|} = \frac{\left(\phi_j - \phi_i\right)\left(\mathbf{r}_j - \mathbf{r}_i\right)}{\left|\mathbf{r}_j - \mathbf{r}_i\right|^2} \tag{15}$$

The right-hand side of Equation (15) is an element of relative positional vector in the "gradient model" as shown in Figure 2, and the gradient vector of particle i is modeled as the following equation by using the particles, which are in interaction area,

$$\langle\nabla\phi\rangle_i = \frac{d}{n_0}\sum_{j\neq i}\left[\frac{\left(\phi_j - \phi_i\right)\left(\mathbf{r}_j - \mathbf{r}_i\right)}{\left|\mathbf{r}_j - \mathbf{r}_i\right|^2} w\left(\left|\mathbf{r}_j - \mathbf{r}_i\right|\right)\right] \tag{16}$$

where d is the number of dimension, n_0 the density of particle number and $w(|\mathbf{r}_j - \mathbf{r}_i|)$ the weighting function. It is considered in this method that the accuracy will be deteriorated when the distribution of particles is arranged in an irregular pattern. We need to study this issue theoretically and numerically as well.

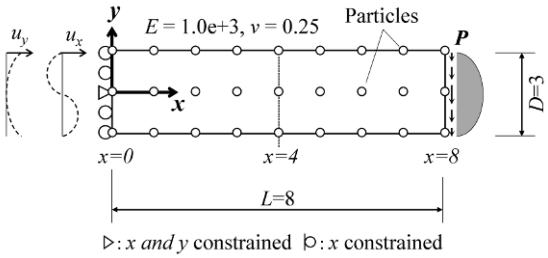

Fig. 3 Timoshenko beam model; particles are regularly located as 8 × 2, 16 × 4, 24 × 6, 32 × 8, 40 × 10, 48 × 12 and 56 × 14

3 Numerical Examples

3.1 Energy Norm in Elasticity Field

Both SPH and MPS are applied to the bending problem of the Timoshenko's cantilever beam in elasticity [23], where the length is 8, the height 2 and the width 1 as shown in Figure 3. This model includes parabolic variation of applied shear traction at $x = L$ with essential boundary condition at $x = 0$ to match the exact solution [24]. In this example, the theoretical displacement fields are given by the following equations:

$$u = -\frac{Py}{6EI} \cdot \left((6L - 3x)\, x + (2 + \nu) \left(y^2 - \frac{D^2}{4} \right) \right) \tag{17}$$

$$v = \frac{P}{6EI} \cdot \left(3\nu y^2 (L - x) + \frac{D^2 x}{4} \cdot (4 + 5\nu) + (3L - x)\, x^2 \right) \tag{18}$$

We assume the plane stress condition with the Poisson's ratio ν of 0.3 and the Young's modulus E of $1.0e + 3$ as the material constants. As shown in Figure 3, we prepare 7 symmetrically arranged nodal patterns: 8 × 2, 16 × 4, 24 × 6, 32 × 8, 40 × 10, 48 × 12, and 56 × 14.

Here, enforcing the theoretical values given by Equations (17) and (18) on the particles, the strain energy values are calculated. In order to study the convergence, the standard deviation of the error norm in energy or S_E is defined as follows:

$$\mathbf{S}_E = \sqrt{\frac{1}{n} \sum_{i=1}^{n} (|e_i| - |\bar{e}_i|)^2} \tag{19}$$

with

$$|e_i| = \sqrt{\left(\varepsilon_i - \varepsilon_i^{\text{exact}}\right)^T \left(\sigma_i - \sigma_i^{\text{exact}}\right)} \tag{20}$$

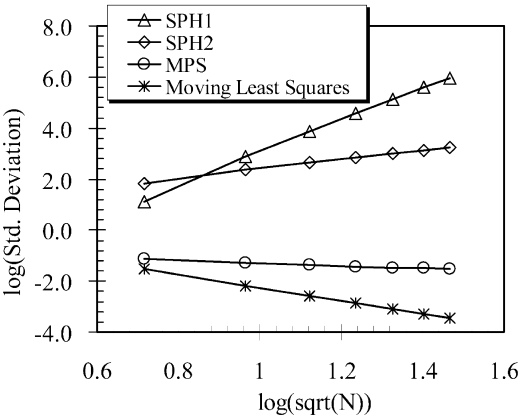

Fig. 4 Standard deviation of energy norm versus numbers of particles, where "SPH1" means the results with Equations (6) and (7), "SPH2" Equations (9) and (10), and "Moving Least Squares method" based on 1st order polynomial approximation

where ε_i and σ_i are the numerical results of strain and stress on particle i, respectively, and $\varepsilon_i^{\text{exact}}$ and σ_i^{exact} the theoretical values of the same, respectively. The latter is given as

$$\varepsilon_x = -\frac{Py}{EI}(L-x) \tag{21}$$

$$\varepsilon_y = \frac{\nu Py}{EI}\cdot(L-x) \tag{22}$$

$$\varepsilon_{xy} = \frac{P}{EI}(1+\nu)\left(\frac{D^2}{4}-y^2\right) \tag{23}$$

It is noted here that the stresses of Equation (20) are calculated by using the stress-strain relationship in elasticity, $\sigma = \mathbf{D}\varepsilon$ (D: stress-strain matrix), as usual.

In this chapter we employ the biquadratic B-Spline function as the weighting function for the SPH method, which is given as

$$w(r_j) = \frac{5}{\pi h^2}\left[1-6\left(\frac{|r_j|}{h}\right)^2+8\left(\frac{|r_j|}{h}\right)^3-3\left(\frac{|r_j|}{h}\right)^4\right] \quad (0 \le |r_j| \le h) \tag{24}$$

where h is the radius of the support of the weighting function, and $|r_j|$ the distance between two points $\mathbf{x}$ and $\mathbf{x}_j$. Regarding the MPS method, the following inverse power weighting functions is chosen:

$$w(r_j) = |r_j|^{-\alpha} \quad (\alpha = 1) \tag{25}$$

Figure 4 shows the analytical results of the standard deviation of the norm in energy versus the numbers of particles, where "SPH1" means the case employing

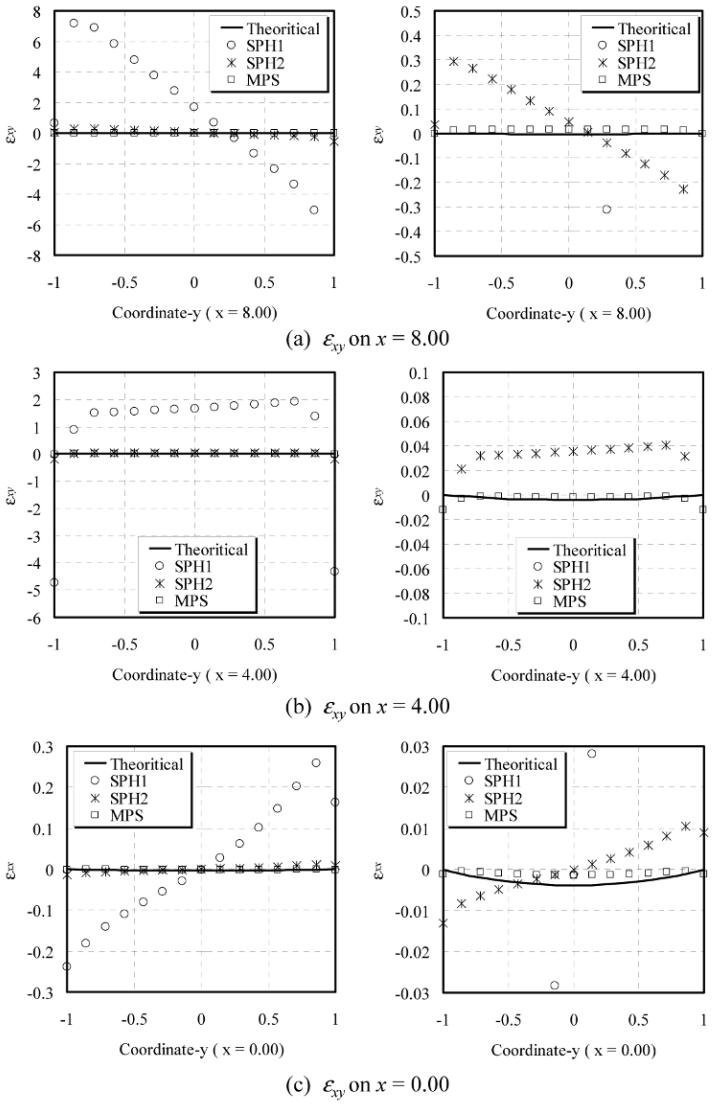

Fig. 5 Comparisons of strain distributions; 56 × 14 particles with regular arrangement (the figures in the right-hand side are the zoomed ones)

Equations (6) and (7) as the SPH discretization, whereas "SPH2" means the case of Equations (9) and (10). The results of moving least squares method [25] based on the 1st order polynomial approximation are also shown in this figure. From this figure, we can see that, although the accuracy of SPH2 is better than that of SPH1, the convergence characteristic of these methods is not satisfactory even if the numbers

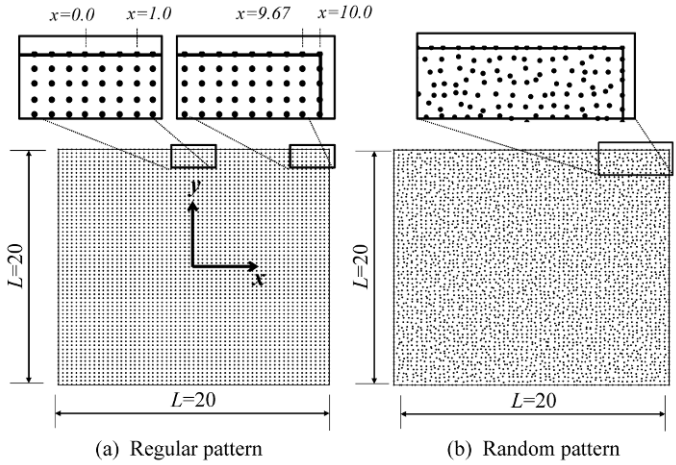

Fig. 6 Two kinds of particle distributions in case of 3721 particles

of particles increase. We consider that this result is due to the fact that the boundary integration is neglected as discussed in Section 2.

On the other hand, the accuracy and convergence of MPS is better than those of SPH1 and SPH2, but worse than those of the Moving least squares method. Then, we examine the distribution of ε_{xy} in the SPH and MPS method in case of 56×14 particles arrangement as shown in Figure 5. It is seen from this figure that, as for the results by all the method except SPH1, some error is observed on the boundaries $x = 8.0$ and 0.0. Particularly, the results of SPH2 methods diverge around these points and those of SPH1 are not agreeable with the exact solution at the whole domain.

3.2 Strain Distributions in Complicated Displacement Field

Let us apply the SPH and the MPS methods to the complex displacement field described as

$$u = \sin\sqrt{x^2 + y^2} \tag{26}$$

$$v = \cos\sqrt{x^2 + y^2} \tag{27}$$

In this example, Equations (26) and (27) are employed as the given displacement vector at the particles, and the calculated strains on the particles are compared with theoretical ones given as follows:

$$\varepsilon_{xx} = \frac{x \cdot \cos\sqrt{x^2 + y^2}}{\sqrt{x^2 + y^2}} \tag{28}$$

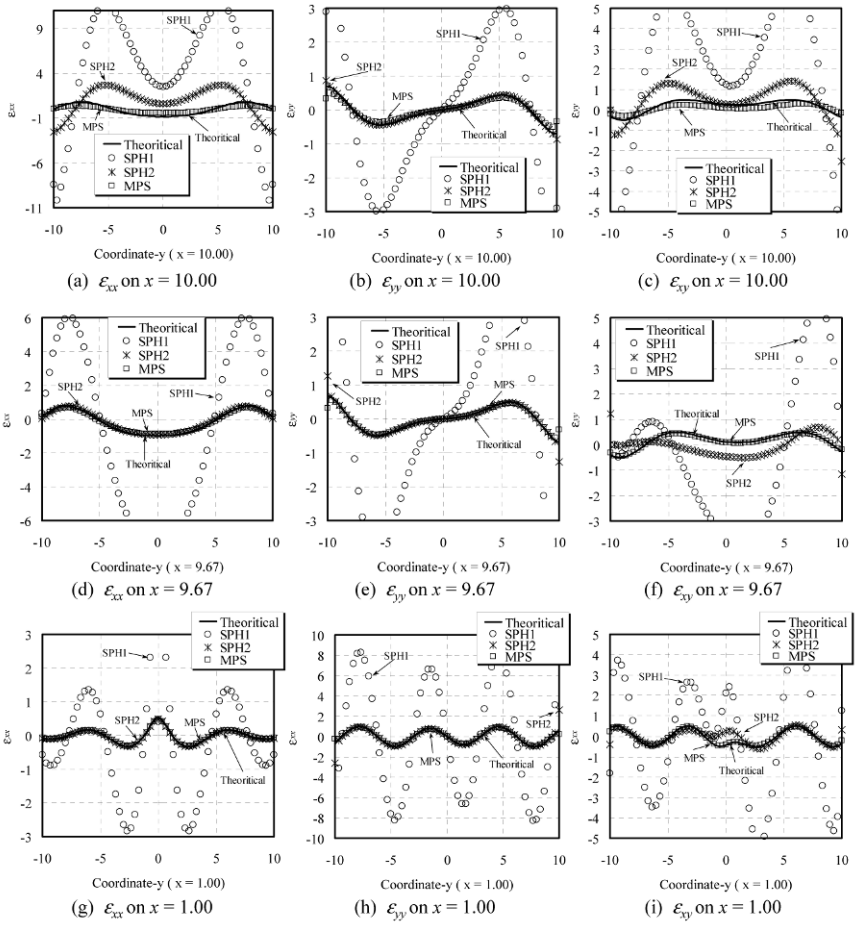

Fig. 7 Comparison of strain distributions; 3721 particles with regular arrangement

$$\varepsilon_{yy} = -\frac{y \cdot \sin\sqrt{x^2+y^2}}{\sqrt{x^2+y^2}} \tag{29}$$

$$\varepsilon_{xy} = \frac{y \cdot \cos\sqrt{x^2+y^2}}{\sqrt{x^2+y^2}} - \frac{x \cdot \sin\sqrt{x^2+y^2}}{\sqrt{x^2+y^2}} \tag{30}$$

In this chapter, the SPH and the MPS methods based on the regular particle pattern and the random one are compared as shown in Figure 6.

Figure 7 shows the calculated distributions of strains ($\varepsilon_{xx}, \varepsilon_{yy}, \varepsilon_{xy}$) by the SPH and the MPS methods in case of the regular particle pattern. From this figure, the distributions of strains are in good agreement with the exact results in the inner area $x = 9.67$ or 1.0 except for SPH1, whereas the results of SPH1 shows deviations from the theoretical ones over the whole domain and the results of SPH2 show

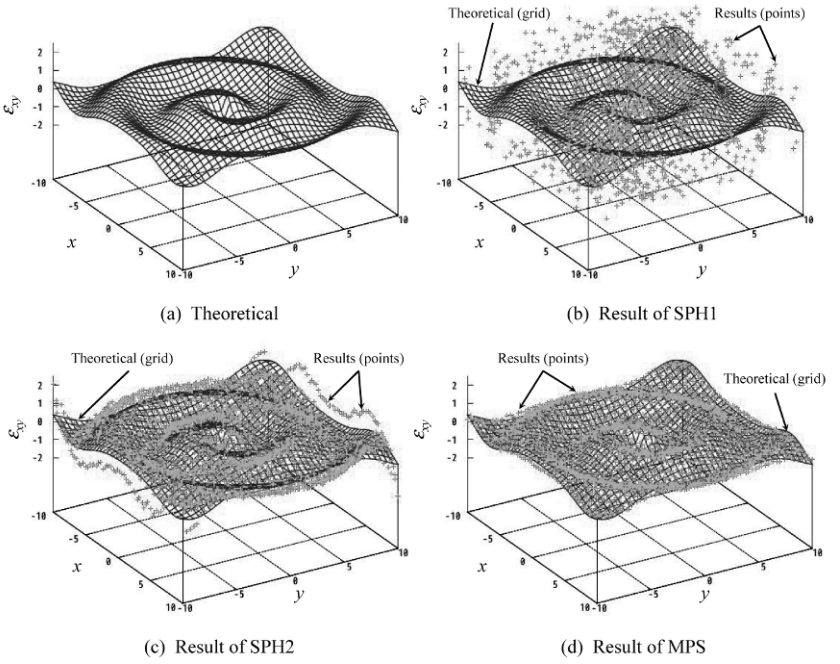

Fig. 8 Comparisons of shear strain distributions; 3721 particles with random arrangement

some deviations from the theoretical ones on the boundary area $x = 10.0$. On the other hand, the results of the MPS method are generally in good agreement with the exact ones even on the boundary area.

Figure 8 shows the calculated distributions of strain ε_{xy} by the SPH and the MPS methods in case of random particle pattern. From this figure, it is seen that the SPH1 gives deviated solutions from the theoretical ones in general, while the SPH2 does large errors only on the boundaries. On the other hand, the results of the MPS are relatively in good agreement with the theoretical ones, but there are also some errors on the boundaries.

4 Conclusion

Discussed in the present paper is the accuracy of the derivative approximation of the particle methods. Especially shown is that the lack of accuracy on the boundary area in the SPH method is due to the lack of the proper boundary integration.

In the numerical examples, we show that, although the accuracy of the SPH2 (modified version of the original SPH) is better than that of the SPH1 (original SPH), the accuracy of both methods is not converged even if the number of particles increases. Furthermore, in the examples of complicated strain fields, we show that,

in case of the random particle pattern, the distributions of strains by the SPH and the MPS methods, especially those of ε_{xy} , are not corresponding to the exact ones.

From the above, it is concluded that more study is needed to re-examine the discretization procedure of the SPH and the MPS methods, especially concerning the discretization of boundaries of the analysis domain.

Acknowledgements

We are grateful to Professor Nakaza and Mr. Iribe, the Disaster Prevention Research Center for Island Regions in University of the Ryukyus for their important contributions to the particle theory.

References

1. Zienkiewicz, O.C., Taylor, R.L., *Finite Element Method*, 5th ed., Vol. 1, Butterworth-Heinemann, Oxford, 2000.
2. Oñate, E., Idelsohn, S.R., Celiguetaa, M.A., Rossia, R., Advances in the particle finite element method for the analysis of fluid-multibody interaction and bed erosion in free surface flows, *Computer Methods in Applied Mechanics and Engineering*, 197(15):1777–1800, 2008.
3. Yagawa, G., Node-by-node parallel finite elements, a virtually meshless method, *International Journal for Numerical Methods in Engineering* 60(1):69–102, 2004.
4. Matsubara, H., Yagawa, G., Convergence studies for Enriched Free Mesh Method and its application to fracture mechanics, *Interaction and Multiscale Mechanics: An International Journal* 2(3):277–293, 2009.
5. Yagawa, G., Matsubara, H., *Enriched free mesh method: An accuracy improvement for node-based FEM*, *Computational Plasticity* 7:207–219, 2007.
6. Tian, R., Matsubara, H., Yagawa, G., Advanced 4-node tetrahedrons, *International Journal for Numerical Methods in Engineering* 68(12):1209–1231, 2006.
7. Li, S., Liu, W.K., *Meshfree Particle Methods*, Springer, Heidelberg, 2007.
8. Lucy, L.B., A numerical approach to the testing of the fission hypothesis, *The Astronomical Journal* 82:1013–1024, 1977.
9. Gingold, R.A., Monaghan, J.J., Smoothed particle hydrodynamics: Theory and application to non-spherical stars, *Mon. Not. R. Astr. Soc.* 181:375–389, 1977.
10. Li, S, Liu, W.K., Meshfree and particle methods and their applications, *Applied Mechanics Review* 55(1):1–34, 2002.
11. Monaghan, J.J., Simulating free surface flows with SPH, *Journal of Computational Physics* 110:399–406, 1994.
12. Belytschko, T., Krograuz, Y., Organ, D., Fleming, M., Krysl, P., Meshless methods: An overview and recent developments, *Computer Methods in Applied Mechanics and Engineering* 139:3–47, 1996.
13. Libersky, L.D., Petschek, A.G., Smooth particle hydrodynamics with strength of materials. In *Advances in the Free-Lagrange Method*, H.E. Trease, M.J. Fritts, W.P. Crowley (eds.), Lecture Notes in Physics, Vol. 395, pp. 248–257, Springer, 1993.
14. Randles, P.W., Libersky, L.D., Smoothed particle hydrodynamics: Some recent improvements and applications, *Computer Methods in Applied Mechanics and Engineering* 139:375–408, 1996.

15. Chen, J.K., Beraun, J.E., Jih, C.J., An improvement for tensile instability in smoothed particle hydrodynamics, *Computational Mechanics* 23:279–287, 1999.
16. Chen, J.K., Beraun, J.E., Jih, C.J., Completeness of corrective smoothed particle method for linear elastodynamics, *Computational Mechanics* 24:273–285, 1999.
17. Chen, J.K., Beraun, J.E., Carney, T.C., A corrective smoothed particle method for boundary value problems in heat conduction, *International Journal for Numerical Methods in Engineering* 46:231–252, 1999.
18. Koshizuka, S., Oka, Y., Moving-particle semi-implicit method for fragmentation of incompressible fluid, *Nuclear Science and Engineering* 123:421–434, 1996.
19. Chikazawa, Y., Koshizuka, S., Oka, Y., Numerical analysis of three dimensional sloshing in an elastic cylindrical tank using moving particle semi-implicit method, *Computational Fluid Dynamics* 9:376–383, 2001.
20. Koshizuka, K., Nobe, A., Oka, Y., Numerical analysis of breaking waves using the moving particle semi-implicit method, *International Journal for Numerical Methods in Fluids* 26(7):751–769, 1998.
21. Iribe, T., Fujisawa, T., Koshizuka, S., Reduction of communication between nodes on large-scale simulation of the particle method, *Transactions of JSCES*, No. 20080020, 2008.
22. Swegle, J.W., Attaway, S.W., Heinstein, M.W., Mello, F.J., Hicks, D.L., An analysis of smoothed particle hydrodynamics, SANDIA Report SAND93-2513, 1994.
23. Timoshenko, S.P., Goodier, J.N., *Theory of Elasticity*, McGraw-Hill, New York, 1979.
24. Augarde, C.E., Deeks, A.J., The use of Timoshenko's exact solution for a cantilever beam in adaptive analysis, *Finite Elements in Analysis and Design* 44:595–601, 2008.
25. Lancaster, P., Salkauskas, K., Surfaces generated by moving least squares methods, *Mathematics of Computation* 37(155):141–158, 1981.